# Passive Seismic Interferometry as a tool for seismic imaging from mine galleries

Hupe, T.; Orlowsky, D.; Draganov, D.

**DOI**
10.3997/2214-4609.202210168

**Publication date**
2022

**Document Version**
Final published version

**Published in**
83rd EAGE Conference and Exhibition 2022

# PASSIVE SEISMIC INTERFEROMETRY AS A TOOL FOR SEISMIC IMAGING FROM MINE GALLERIES

T. Hupe[1,2], D. Orlowsky[2], D. Draganov[3]

[1] Ruhr University of Bochum; [2] DMT GmbH & Co. KG.; [3] Delft University of Technology

## Summary

To test passive seismic interferometry (PSI) in underground mining environments, we carried out an active-source seismic and continuous noise measurement in a mine gallery of a former radioactive waste repository - the Asse II salt mine (Lower Saxony, Germany). To analyze the active-source data, we process the data inspired by conventional seismic processing techniques. On the contrary, for the passive-source data, we first perform an illumination diagnosis to identify and separate seismic wave types. Subsequently, we apply PSI by cross-correlation for the retrieval of body-wave arrivals and finally apply selective-stacking. In this context, we refine processing procedures for PSI inside of mine galleries and point out that data recordings of <24 h and summation times of 10 min to 30 min during selective stacking are sufficient when applying PSI to underground noise data. Using PSI imaging results, we identify several pre-known and unknown geological structures exceeding the number and distance of structures determined from active-source imaging results. Here, PSI showed advantages over the active-source seismic data regarding resolution, energy distribution, and spatial extent.

**Passive Seismic Interferometry as a tool for seismic imaging from mine galleries**

## Introduction

Energy transition from fossil fuels to green technologies is more required than ever. Governments push this process with subsidies and research possibilities. There is, however, a major obstacle. Alternative sources of energies require access to other raw materials and special minerals. The growing demand for minerals and their commonly complex extraction procedures increase the need for affordable exploration techniques. Usually applied methods are large-scale reflection seismic surveys or drilling procedures. Both are time-consuming, expensive, and do not always provide a satisfactory resolution of the subsurface structures. Hence, underground seismic surveys from mine galleries might be a reasonable alternative to obtaining high-resolution data of the subsurface. Several studies have shown that underground reflection seismic imaging in the form of In-Seam Seismic (Schott and Waclawik 2015), horizontal seismic profiling (Dickmann 2014) or conventional reflection seismics (Orlowsky et al. 2018) provide reliable and good results.

However, underground seismic surveys are rare because of their complexities concerning safety, staff education, equipment requirements, timing, and planning. To minimize the reliance on these complexities, active-source seismic techniques could be replaced by the application of Passive Seismic Interferometry (PSI). PSI is a method to retrieve virtual source responses by cross-correlating ambient seismic noise signals at different receiver locations (Wapenaar and Fokkema 2006). Although PSI is a common method for several applications at the surface, a limitted amount of results are shown applying this technique in underground mines. To fill that gap, we carried out both underground passive and active-source seismics to compare the application of PSI by cross-correlation ($PSI_{CC}$) with the use of active-source seismic imaging.

## Test Site

Data acquisition was performed between October 22 and November 12, 2019, in a mine gallery of a former German salt mine and nuclear waste repository - the Asse II mine. The mine is currently operated by the federal company for radioactive waste disposal, and is located approximately 70 km south-east of Hanover at the western end of the 25-km-long, NW-SE trending Asse-Jerxheim salt structure. The Asse-Jerxheim salt structure is part of the western Subhercynian Basin built up by anticlinal-uplifted Late Permian Zechstein evaporites and Triassic sediments (Pollok et al. 2018). Within the complex internal structure and composition of the Asse-Jerxheim salt structure, initially, flat-bedded Zechstein evaporites developed to a salt pillow in the Jurassic and were compressionally deformed in the Late Cretaceous. Shortening, accompanying the inversion, led to intrusion of the Zechstein salt dome into the southwestern part of the Triassic overburden forming a "salt wedge". Hence, at its southwestern flank, the salt wedge is joined to the geological units of the Triassic Upper Buntsandstein (Pollok et al. 2018).

## Geometrical Layout

The geometrical layout for our tests included a receiver line with a total of 35 three-component receiver probes. The probes were inserted in vertically drilled boreholes having a diameter of 65 mm, a depth of 2.5 m, and a spacing of 4 m at the floor along a 140-m-long, abandoned gallery section of the mine. **Figure 1** shows the floor plan of the 574-m-deep mine gallery with the receiver and source positions of the passive and active-source seismic data acquisition. Seismic signals for the active-source acquisition were generated by vertical sledgehammer blows at the gallery floor and at the gallery side-wall opposing the receiver layout. The blows were carried out next to and in between every receiver position.

The recording time was set to 500 ms with a sample rate of 0.5 ms. The blows were stacked four times at each source position. For applying PSI, a total of 156 h of continuous ambient-noise data, stored in 60-second-long compartments with a sample rate of 1 ms, were recorded. We processed and evaluated 24 h of coherent data consisting of the X-, Y-, and Z-component of all 35 receivers concatenated in one noise panel (105 channels). We chose these 24 hours following a visual data review evaluating the amount of apparent seismic events and visible signal-to-noise ratio.

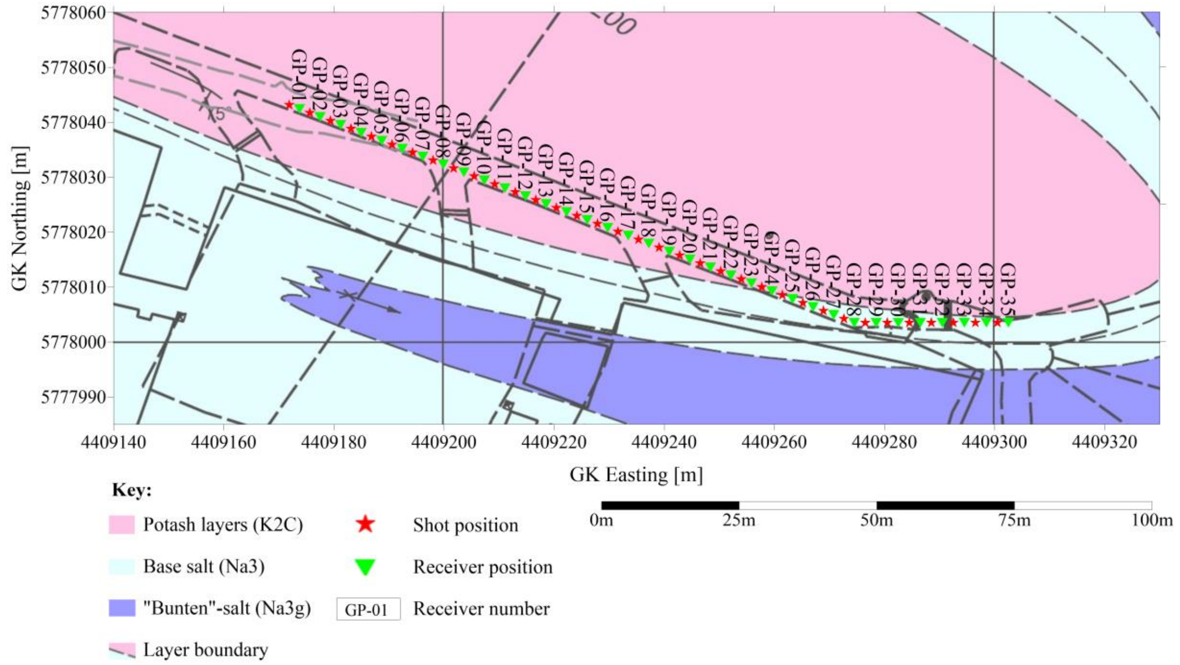


***Figure 1*** *Floor plan of the 574-m-deep mine gallery including the geometrical layout for the underground seismic acquisition.*

**Methods and Results**

Each recorded seismic data set, passive and active, is processed differently to obtain optimal seismic imaging results. While the active-source data are processed according to a hybrid processing flow inspired by Dickmann (2014), we separate the passive-source data into its X-, Y-, and Z-components as well as summing the 60-s-long noise panels to generate one 24-h-long noise panel. Then, after some filter tests on pre-correlated and post-correlated data, we choose a frequency band of the passive seismic data between 15 Hz and 250 Hz.

According to the pre-processing, we apply $PSI_{CC}$ to retrieve sources from seismic noise signals at different receiver locations. $PSI_{CC}$ is based on the retrieval of the Green's function between two points. The Asse salt structure comprises different inhomogeneous evaporitic units. The mine gallery is surrounded by noise sources from mine ventilation, high voltage boxes, or drilling machines.

We normalize the amplitudes of one noise panel and cross-correlate each of the traces component-wise with a so-called master trace (e.g., first receiver in a noise panel) within a 60 s correlation window. This relatively short correlation window was applied according to a known reflector (salt limit) in about 300 m distance to the geophone layout. To separate the travel-time of the direct arrival from the travel-time of its multiple and to retrieve the desired reflection from cross-correlation, the correlation window should be longer that the expected two-way travel-time of seimic signals reflected at the furthest reflector of interest. As we target the extraction of reflectors to create a suitable image of the subsurface, we apply an illumination diagnosis following Vidal et al. (2014) to exctract preferential illumination by body waves. In general, the illumination diagnosis evaluates both body- and surface-wave arrivals passing through the virtual-source position of a correlation panel at t=0 s, forming the virtual source function (Vidal et al. 2014).

We compute the illumination diagnosis for each correlated noise panel to evaluate the dominant seismic wave type of a noise panel. If the maximum amplitude corresponds to predefined slowness limits of body waves, the correlation panel is used for further estimation of the SI response. We choose slowness limits using the body-wave velocities obtained from the active seismic data (P-waves: 4400 m/s to 4600 m/s, S-waves: 2100 m/s to 2300 m/s). **Figure 2** shows exemplary results of the illumination diagnosis for the X-component. Magenta crosses indicate determined slowness values. While the X- and especially the Y-directions are dominated by S-wave arrivals, body waves seem to arrive rather diverse in the Z- direction. In all directions, the surface waves seem to be insignificant, forming the foundation for a further division of body waves into P- and S-waves during the illumination diagnosis.

Subsequently, we further process the pre-seclected body-wave data with PSI. Cross-correlation sections are generated for different master-trace positions, and separately summed over a desired time interval. Using stacking tests of different summation lengths, we identify summation ranges of 10 min to 30 min to be optimal for generating summed common-source gathers. Longer summation windows do not improve the signal quality, but increase the occurrence of artefacts. Subsequently, to generate stacked seismic sections, we firstly form common-midpoint (CMP) gathers by resorting the retrieved data, secondly perform an interactive velocity analysis on these CMP gathers via semblances, and finally apply a normal move-out correction to stack the traces of the CMP gathers. We do this for every receiver component individually. In a last step, we combine the stacked CMP gathers of each receiver component to increase the reflection amplitudes. **Figure 3** illustrates the comparison between a stacked depth section of a) PSI and b) the active-source results with identiefied reflectors ($PSI_{CC}$ – green, active-source – black) projected on the geological floor plan of the 574-m-deep mine gallery. The projected limit of the salt dome is displayed as a yellow marked reflector.

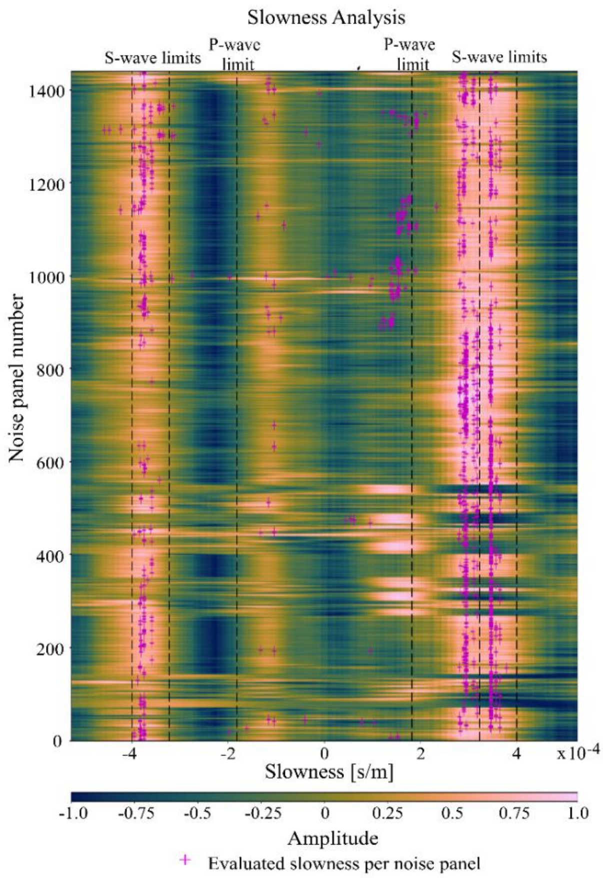


***Figure 2** Results of the Illumination diagnosis for the X-component.*

After data analysis and interpretation on basis of the geological model, we detect a variety of reflectors north-westerly from the receiver layout. With the aid of the geological floor plan of the mine, we assign these reflectors to geological interfaces (**Figure 3**). The application of PSI yields maximum distances of reflectors of about 500 m, whereas the results of the active seismic method show reflectors with maximum distances up to about 400 m. This is based on the fact, that the active seismic is limited to the source energy, the source positions, and the source-energy distribution.

**Conclusions**

We tested the application of passive seismic interferometry (PSI) in a mine gallery and compared the results to results from active-source data. We refined the PSI processing steps for their use in mine galleries. The PSI-related illumination diagnosis revealed that noise sources, particularly in the Asse II mine, appear to be homogeneously distributed. Noise data are dominated by body waves and their superposition with surface waves is neglectable. Subsequent stacking of the noise data showed that the summation of data for time windows >30 min did not improve the signal-to-noise ratio, but rather increased the occurance of artifacts and ghost reflections. After further quantitative and qualitative data processing and analysis of the active- and passive-source data sets, we verified pre-known structures as well as detected unknown reflectors with the aid of PSI. The gained resolution was comparable to the use of active-source data. Applying PSI even seems to be beneficial concerning the number of identified reflections, the spatial range, and the source distribution compared to an active-source seismic acquisition using a sledgehammer.

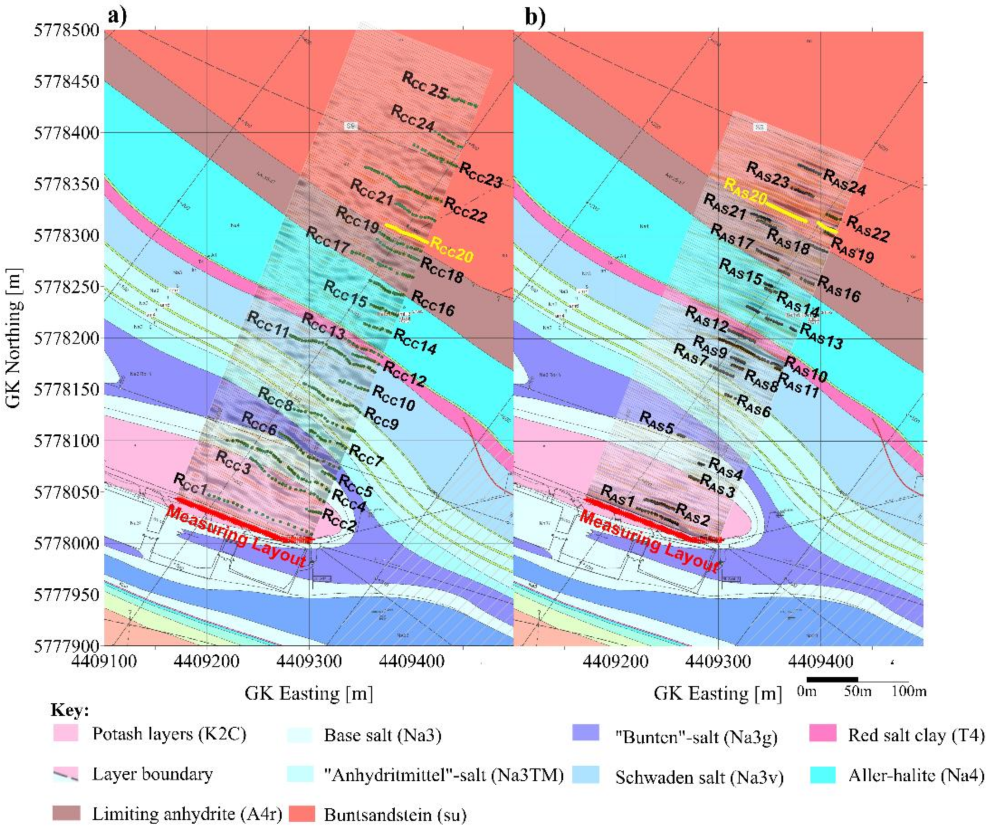


***Figure 3*** *Reflectors extracted from **a)** PSI (green) and **b)** the active seismic evaluation (black), projected on a 2D section of the geological model of the Asse II mine in the surrounding of the 574-m-deep gallery. The yellow reflector displays the projected limit of the salt dome.*

**Acknowledgments**

Funding for this research was provided by the EIT Raw Materials and DMT GmbH & Co. KG. We are very thankful to the BGE (Bundesgesellschaft für Endlagerung) to allow the measurement in the Asse II mine. We are very thankful to the whole SIT4ME consortium including Alireza Malehmir and Alba Gil de la Iglesia of the University of Uppsala, Ramon Carbonell, Puy Ayarza, Yesenia Martinez and Juan Alcade of the CSIC in Barcelona and Stefan Buske of the University of Freiberg for their support during planning and implementation of the measurements.

**References**

Dickmann, T. [2014] 3D Tunnel Seismic Prediction: A Next-Generation Tool to Characterize Rock Mass Conditions Ahead of the Tunnel Face. *Journal of Rock Mechanics & Tunnelling Technology*, **20**, 35–47.

Orlowsky, D., Limbrock, K., Lehmann, B. and Peak, A. [2018] The Investigation of the Geological Situation in the Environment of Active Salt Mines Applying Seismic Techniques. *80th EAGE Conference and Exhibition 2018*. EAGE Publications BVNetherlands.

Pollok, L., Saßnowski, M., Kühnlenz, T., Gundelach, V., Hammer, J. and Pritzkow, C. [2018] Geological exploration and 3D model of the Asse salt structure for SE expansion of the Asse II mine. *Mechanical Behavior of Salt*, **IX**, 753–763.

Schott, W. and Waclawik, P. [2015] On the quantitative determination of coal seam thickness by means of in-seam seismic surveys. *Canadian Geotechnical Journal*, **52**(10), 1496–1504.

Vidal, C.A., Draganov, D., van der Neut, J., Drijkoningen, G. and Wapenaar, K. [2014] Retrieval of reflections from ambient noise using illumination diagnosis. *Geophysical Journal International*, **198**(3), 1572–1584.

Wapenaar, K. and Fokkema, J. [2006] Green’s function representations for seismic interferometry. *GEOPHYSICS*, **71**(4), SI33-SI46.